

NUMERICAL AND EXPERIMENTAL CHARACTERIZATION OF A RAILROAD SWITCH MACHINE

Dario Croccolo^(*), Massimiliano De Agostinis, Stefano Fini, Giorgio Olmi

Department of Industrial Engineering, University of Bologna, Italy

^(*)Email: dario.croccolo@unibo.it

ABSTRACT

This contribution deals with the numerical and experimental characterization of the structural behaviour of a railroad switch machine. Railroad switch machines must withstand a number of safety related conditions such as, for instance, the appropriate resistance against any undesired movements of the points, due to the extreme forces exerted by a passing train. This occurrence can produce a very high stress on the components that has to be predicted by designers. In order to assist them in the development of new machines and in defining what are the critical components, FEA models have been built and stresses have been calculated on the internal components of the switch machine. The results have been validated by means of an ad-hoc designed experimental apparatus, now installed at the facilities of the Department of Industrial Engineering of the University of Bologna.

Keywords: railroad switch, railway junction, FEA, experimental, points.

INTRODUCTION

A railroad switch machine (RSM), turnout or set of points is a mechanical installation enabling railway trains to be guided from one track to another, such as at a railway junction or where a spur or siding branches off. One of the key safety requirements of railroad switches is related to achieving a suitable resistance against any undesired movements of the points, due, for instance, to the extreme forces exerted by a passing train in the case of the needle leaned to the rail (force F in Fig. 1).

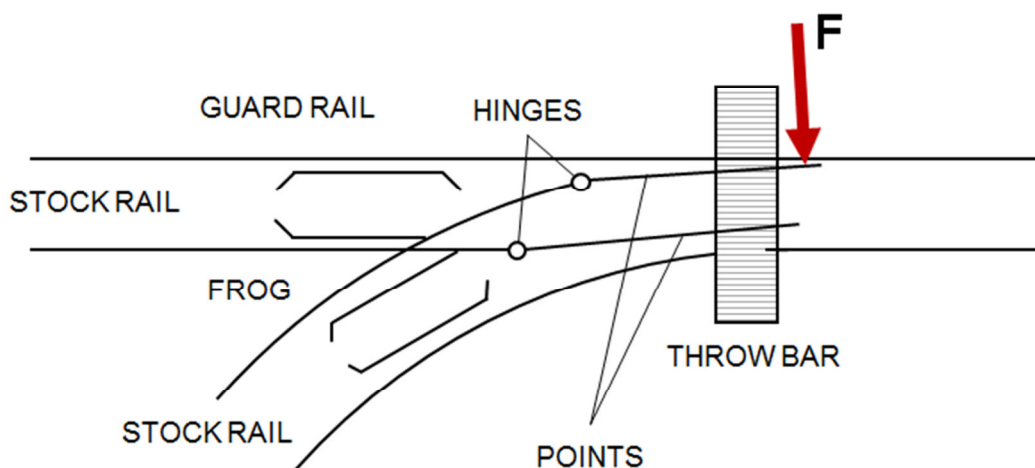


Fig. 1 - Geometry of a railroad switch

Many railway companies assume a force $F=100\text{kN}$ as a standard. This work deals with the development of FEA models aimed at accomplishing the structural design of the RSM under the aforementioned operating load. In order to validate such models, an experimental test bench has been designed and manufactured. This comprises two ad-hoc designed fixtures which allow accommodating the test piece on a standard INSTRON 8500 500kN standing press and applying forces up to a maximum of $F=300\text{kN}$.

MATERIALS AND METHODS

The Alstom RSM object of the present investigation is shown in Fig. 2, along with some balloons highlighting the key structural components of the machine.

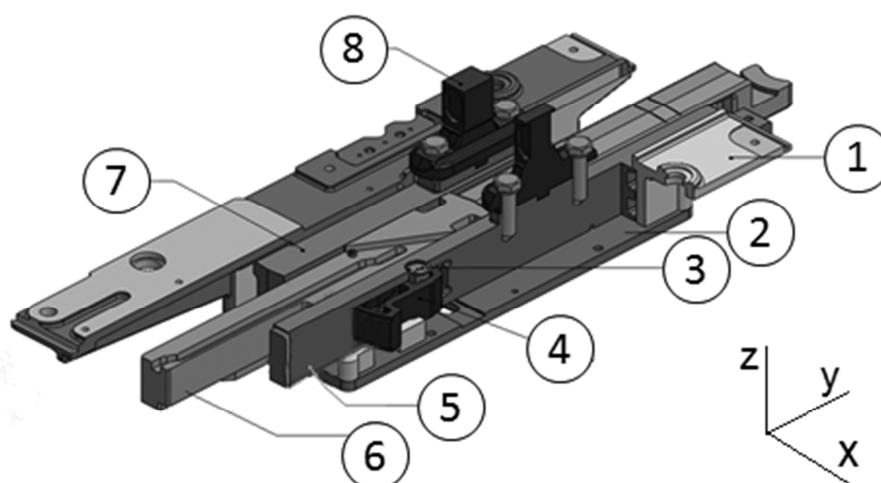


Fig. 2 - 3d model of the Alstom RSM: (1) body, (2) lower plate, (3) pin, (4) hammer, (5) switching rod, (6) cam, (7) detection rod, (8) arm

Due to confidentiality related issues, the working principles of the machine cannot be described in detail. The analysis was limited to the verification of the mechanism against unwanted movements of the points caused by a passing train since the system is equipped with two interlocking devices. In fact, once the full stroke has been travelled, and the points are in the open (or closed) position, the switching rod (5) is secured to the body (1) by means of a hammer (4); at the same time, the detection rod (7) is secured to the lower plate (2) by means of a slider, not represented in the picture. Therefore the locking devices come into effect preventing any movement of the rods, when an external force is applied along z-axis to the points, and thereby to the arms (8).

According to the requirements set by railway companies, the RSM shall be validated under the action of a force $F=100\text{kN}$. In order to attain an adequate stiffness of the test fixture, it has been dimensioned for a maximum load of 300kN . The overall dimensions of the test piece are $900 \times 300 \times 210\text{mm}$, therefore the fixture has been conceived in two separate parts, a lower and an upper grip, so as to achieve a certain flexibility during mounting and unmounting operations on the standing press. In order not to transmit any unwanted bending moment at the arms, the test fixture is shaped as shown in Fig. 3.

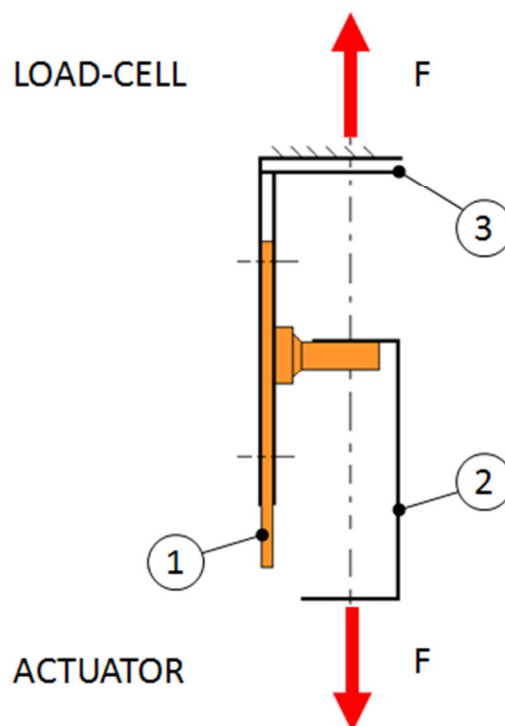


Fig. 3 - Loading scheme: (1) test piece (switch machine), (2) lower grip, (3) upper grip

While the lower grip is a simple C-shaped interface between the actuator thread and the arms, the upper grip has to retain the whole RSM by means of four M20 8.8 class bolts. The bolted joint is doubly overlapped: this provision allows doubling the frictional surfaces and hence the transmissible load for given bolt size and class [1-2]. Except for a few details, the fixture has to be arc welded, therefore a structural steel S275JR according to [3] has been chosen for its construction. All the welds have been statically dimensioned according to Standard EN 1993-1-8 [4]. In order to assess the stresses and the deformations on the fixture under maximum design load ($F=300\text{kN}$), some FEA have been performed by means of the commercial code Ansys Workbench.

Fig. 4 (a) shows the boundary conditions applied to the model: the upper grip has been fixed at the upper end and loaded by two equal forces $F_z=150\text{kN}$, one at each arm. The model has been meshed with SOLID187 Tetrahedral and Hexahedral elements, Fig. 4 (b), for a total node count of about 80,000 nodes. The material is a structural steel with $E=200\text{GPa}$ and $\nu=0.3$, whereas the bonded contacts are managed by means of the pure penalty contact algorithm, with the normal stiffness factor set to $FKN=0.01$, following the lines suggested by [5]. As it can be appreciated by looking at Fig. 4 (c) the total deformation is $\Delta_{\text{tot_max}}=1.3\text{mm}$ whereas the maximum von Mises equivalent stress remains below 190MPa (see Fig. 4 (d)); such a stress level is well below the material yield point $S_Y=275\text{MPa}$. Since the model is linear, a maximum deformation of about $\Delta_{\text{tot_nom}}=0.4\text{mm}$ can be expected at nominal load, which is deemed as acceptable.

The assembly procedure of the test rig requires quite a number of subsequent operations, briefly summarized in Fig. 5. Particularly, Fig. 5 (d) shows the detail view of the arms of the machine when these are clamped by the lower grip. When the assembly is done, the load cell undergoes zero calibration and the test can begin. The main target of the experimentation is to provide a validation of FEA models of the RSM that will be described in the following. A

secondary aim of the experimentation is to determine how much of the total load is borne by the switching rod and how much by the detection rod. In order to accomplish this twofold task, three components of the RSM have been instrumented by strain gauges: the two arms and the pin (see Fig. 6).

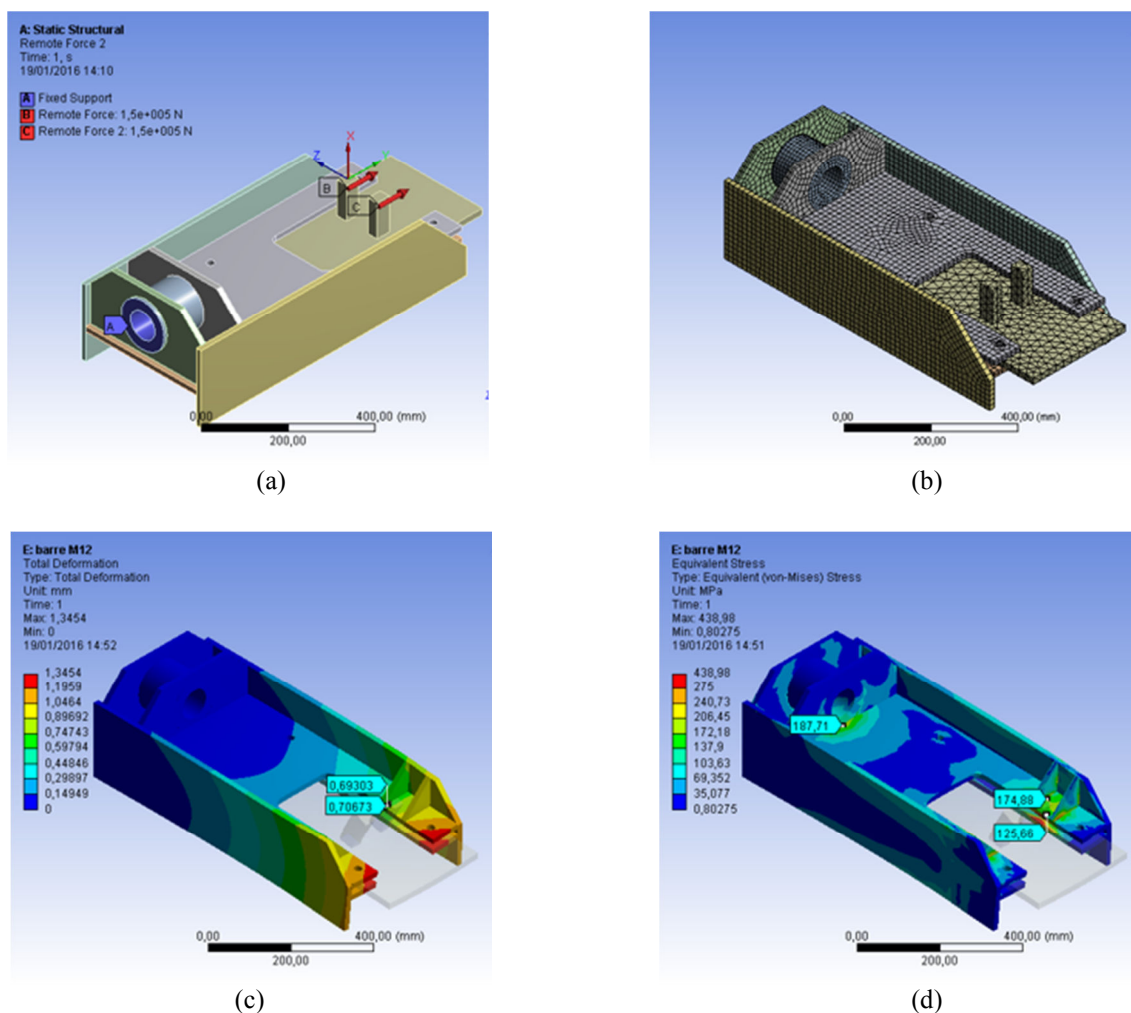


Fig. 4 - FEA on the fixture upper grip: (a) Boundary conditions, (b) mesh, (c) total deformation, (d) equivalent von Mises stress

Pin and arms have been previously reworked in order to accommodate the sensors (Vishay Precision Group J2A-XXS047K-350): particularly, the pin required both milling and boring operations in order to achieve a plane surface for the application of the strain gauge as well as a passage for the cables. The arms have been instrumented by means of two strain gauges each: the strain gauges were connected in a half bridge fashion to the Wheatstone circuit. The pin has been instrumented by means of a single strain gauge: a dummy gauge, which served as a temperature drift compensator, was glued to an identical, unloaded pin placed in the testing room. The adhesive used for the installation was the M-BOND 200 by Vishay Precision Group. All the sensors have been installed by a certified operator, following the lines suggested by Standards [6-8]. The data acquisition has been managed by means of the NI 9237 sampling card plugged into a NI cDAQ-9184 carrier.

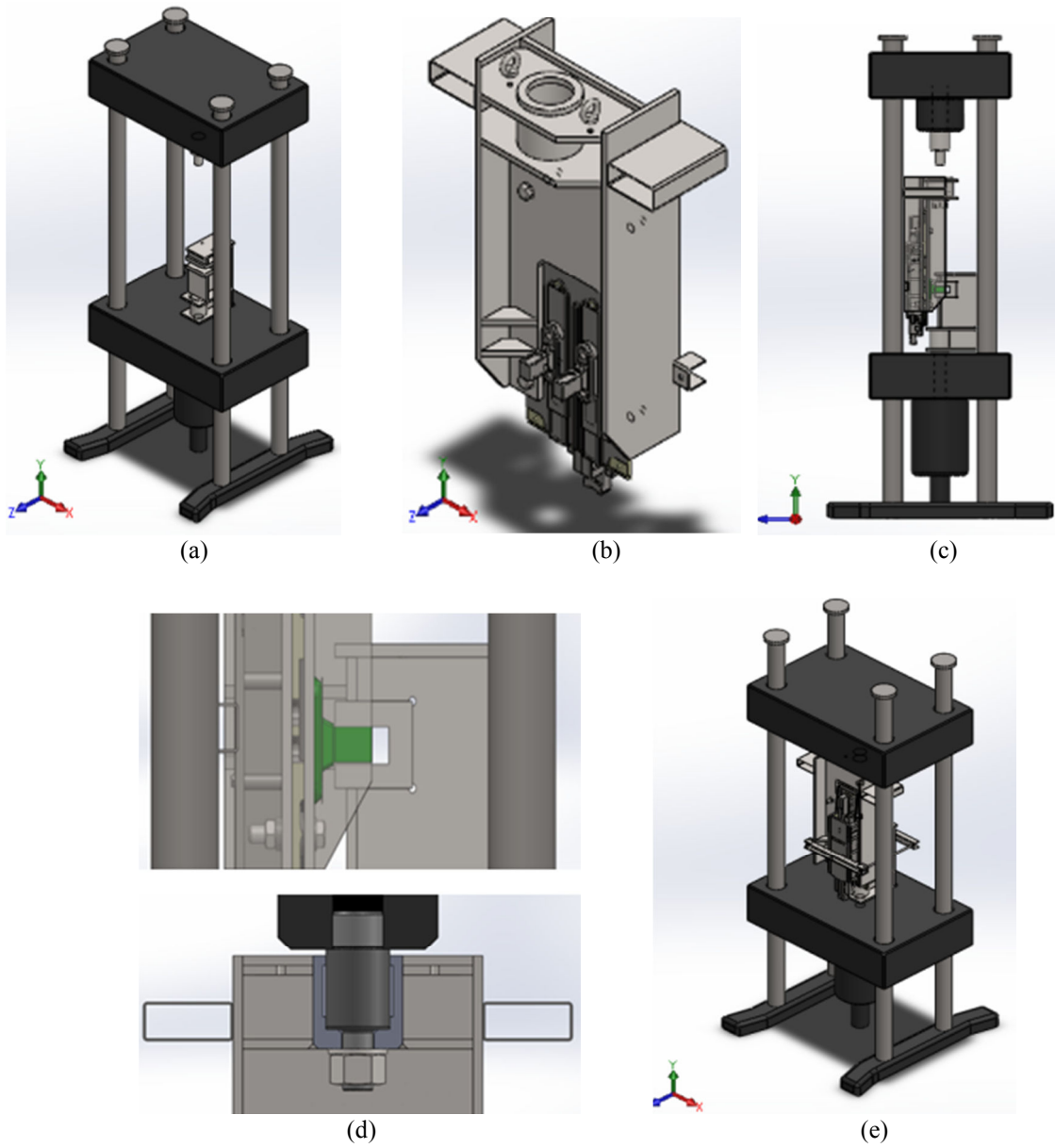


Fig. 5 - Test arrangement: (a) Placement of the lower grip, (b) pre-mounting of the upper grip with the test piece, (c) placement of the upper grip with a forklift, (d) details of the assembly, (e) final configuration

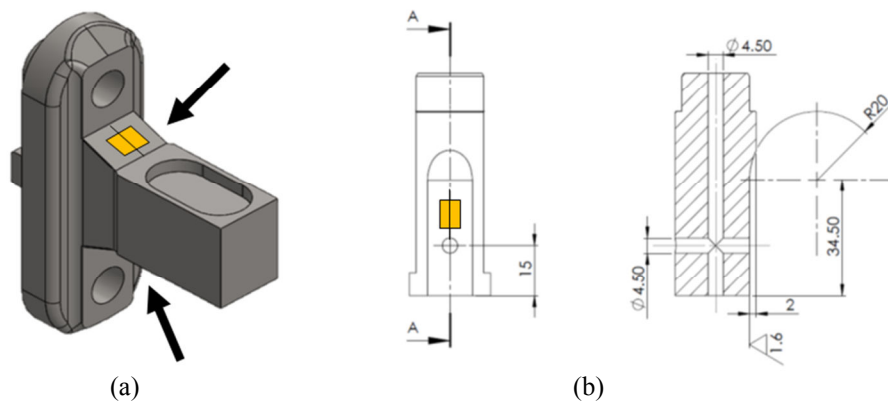


Fig. 6 - (a) Placement of the strain gauges on the arm and (b) on the reworked pin

The FEA model of the RSM has been developed by means of the Ansys code V.17. Due to the complexity of the assembly, submodeling has been leveraged, by considering half a model at a time, as if the machine were cut along its mid-plane, normal to x-axis. Doing this way, it has been possible to find a satisfactory balance between accuracy and computational cost. Both the models have been meshed with tetrahedral elements SOLID187, for a total node count of 360,000 nodes in the case of the switching rod side (Fig. 7), and 485,000 nodes for the detection rod side (Fig. 8). In the case of the switching rod, the stresses on the pin and those on the hammer have been sampled, and subsequently compared with the experimental outcomes. In the case of the detection rod, the stresses on the pins which connect the lower plate to the body have been examined, as a function of the actual bolt preload of the joint.

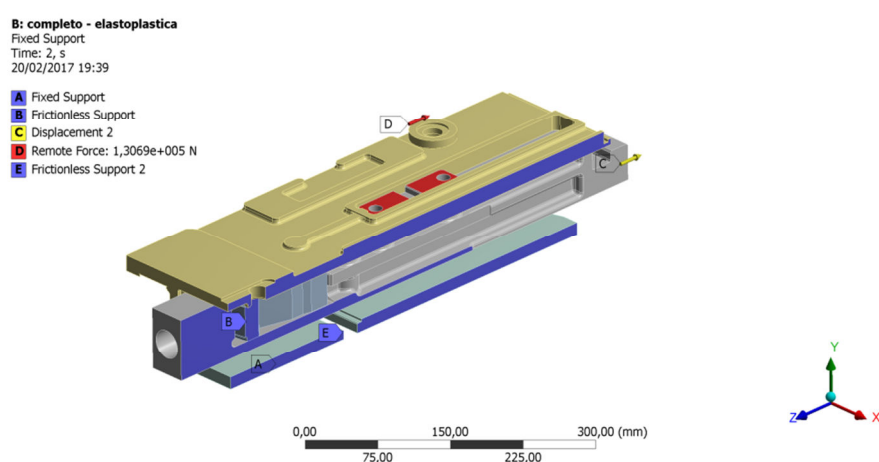


Fig. 7 - Boundary conditions for the half model comprising the switching rod

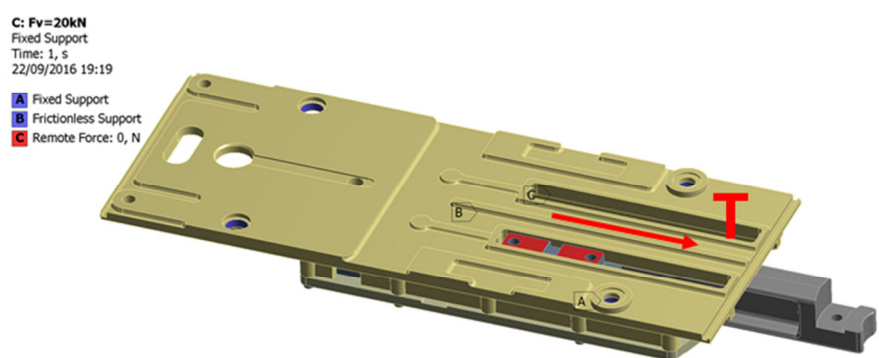


Fig. 8 - Boundary conditions for the half model comprising the detection rod

RESULTS AND CONCLUSIONS

The results from a tensile test carried out on the ad-hoc developed test bench are shown in Fig. 9. This reports the data relevant to a test run until a maximum force of $F=160\text{kN}$. At the peak load, one of the pins connecting the lower plate with the body failed. The first outcome of the experimentation is the knowledge of the force distribution on the two arms: the great majority of the total force (82%) reaches the body by passing through the chain of components named the switching rod, the pin and the hammer. The remaining part (18%) passes through the detection rod, the slider and the lower plate, eventually reaching the body.

Running each of the FEA models by applying the appropriate fraction of the total load to the arm under investigation, it has been possible to validate the numerical results.

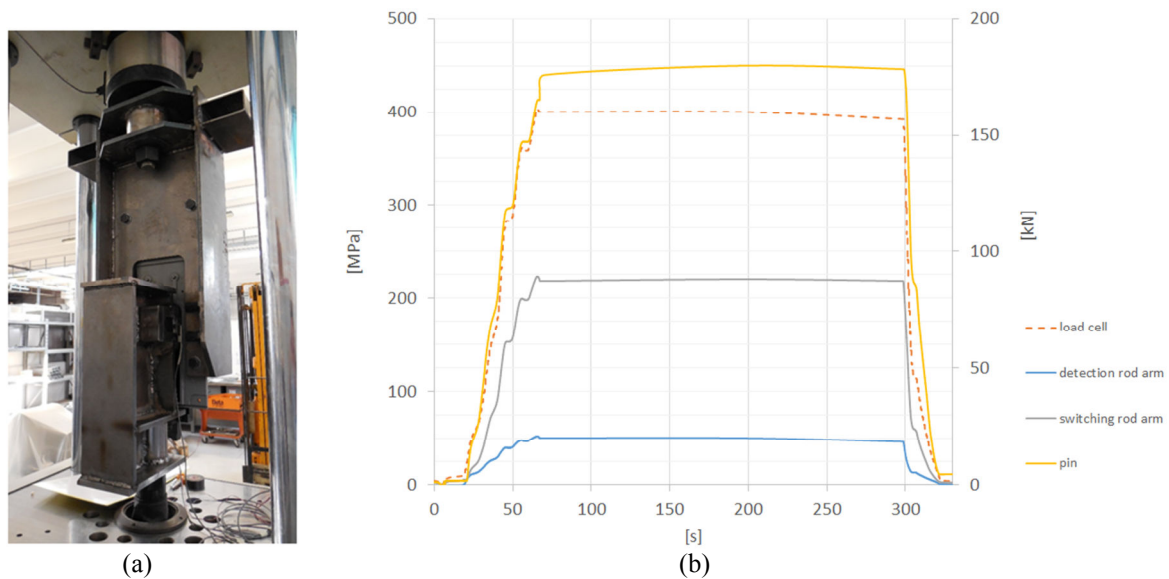


Fig. 9 - (a) View of the test bench and (b) plot of the results in terms of stresses on the pin and on the arms and force at the load cell.

For example, looking at Fig. 10 (a), it is possible to observe the equivalent stresses calculated according to the von Mises criterion on the half machine comprising the switching rod. Fig. 10 (b) reports the σ_Y bending stresses on the pin that supports the hammer, when this sub-system is loaded with 82% the total load $F=160\text{kN}$.

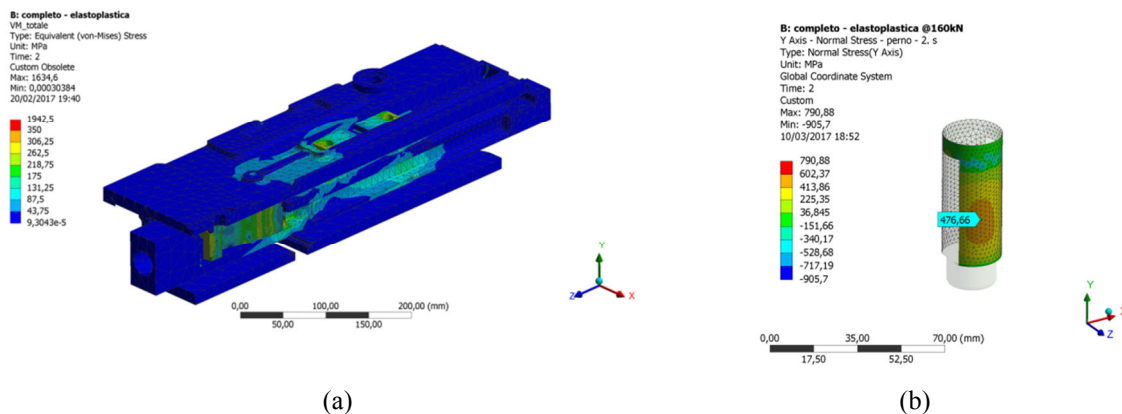


Fig. 10 - (a) von Mises stress plot on the half machine - switching rod side and (b) bending σ_Y stresses on the pin

As it can be appreciated from Fig. 10 (b), the numerical peak of the bending stress on the pin ($\sigma_{Y_FEA}=477\text{MPa}$) is very close to that measured during the experimental test on the same component ($\sigma_{Y_EXP}=450\text{MPa}$, see Fig. 9). The error, calculated according to Eq. (1), is acceptable.

$$e\% = \frac{\sigma_{Y_FEA} - \sigma_{Y_EXP}}{\sigma_{Y_EXP}} \cdot 100 = 6\% \quad (1)$$

Once the FEA model has been validated, it can be used for carrying out some comparisons considering, for example, the joint between the lower plate and the body. Such joint comprises a pattern of eight M8 8.8. screws, working in parallel with a couple of parallel pins of $d=6\text{mm}$ diameter, manufactured according to Standard [9]. It can be assumed that this joint must withstand the shearing load transmitted by the slider to the body via the lower plate. Since the screws are tightened under preload control upon assembly, and some uncertainties on the friction coefficients cannot be avoided [10-12], the load borne by the parallel pins may vary depending on the effective preload of the screws and on the friction coefficient at the interface between the body and the plate. In order to estimate such variation, some parametric analyses have been run, for example by imposing different preload levels to the screws. The screw preload has been assigned via the preload tool available in the Ansys Workbench environment.

Fig. 11 reports a plot of the amount of shearing force borne by the switching rod side pin (T'_{swi}) and by the detection rod side pin (T'_{det}) as functions of the actual screw preload F_v . Each of the dashed lines represents the force acting on the relevant parallel pin, whereas the solid lines represent the fraction of load borne by the generic pin.

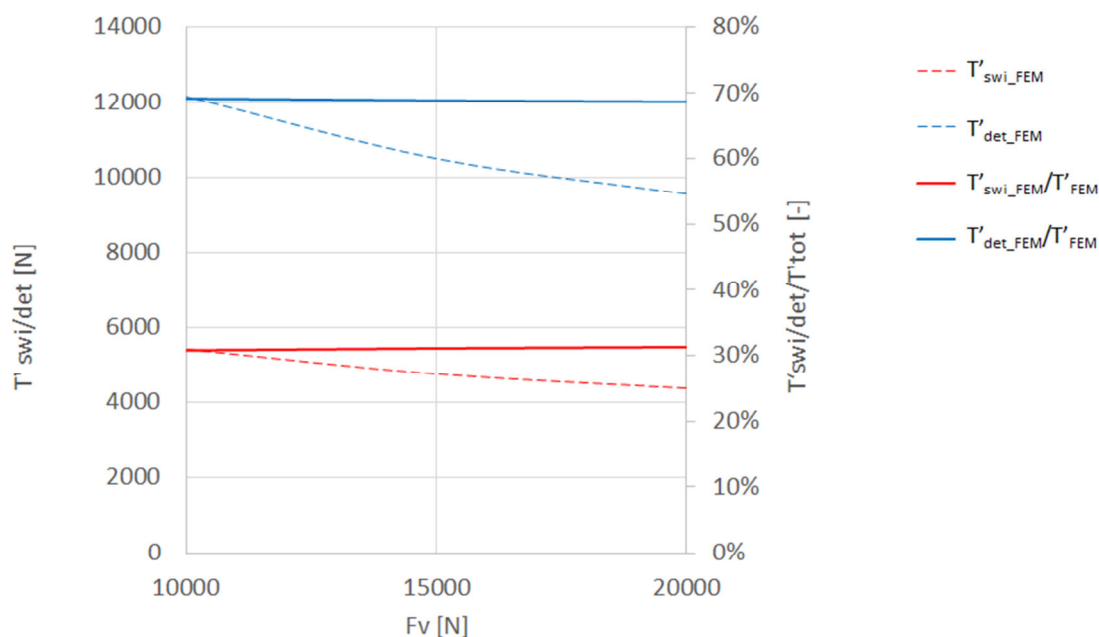


Fig. 11 - Shearing force on the switching/detection rod side parallel pin versus screw preload.

It can be seen that the most loaded pin is that on the detection rod side (closer to the slider), regardless the screw preload. Nonetheless, the magnitude of the load borne by the pins decreases as the screw preload increases: the preload limit of $F_v=20\text{kN}$ is assumed based on the provisions of Standard [13] for M8, 8.8 class screws. Based on different preload levels, it is also possible to extract a plot of the von Mises stresses on the most loaded parallel pin, as shown in Fig. 12.

The equivalent stress calculated by FEA on the most loaded parallel pin is compatible with the failure event, which took place during the experimentation, at a total load of $F=160\text{kN}$.

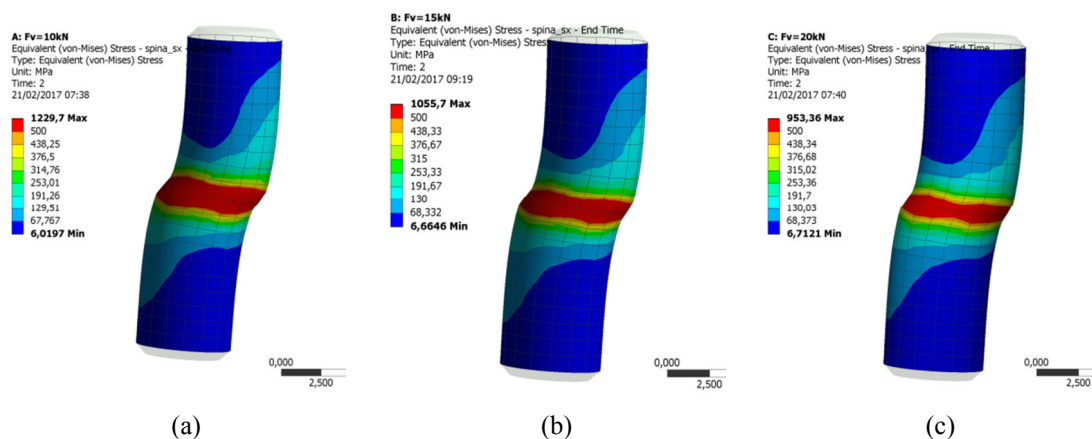


Fig. 12 - von Mises stress plot on the detection rod side parallel pin at screw preload of (a) 10kN, (b) 15kN, (c) 20kN

From the designer's standpoint, the present work achieved a twofold result: (i) an experimental setup has been designed, manufactured and calibrated, which will be useful for subsequent experimentations on other products of the same family; (ii) numerical tools have been developed and validated, with respect to experimental data. These models allow the designer early evaluating the effect of structural changes, hence reducing the time to market of new machines.

ACKNOWLEDGMENTS

The authors gratefully acknowledge Eng. Marcello Andrenacci, Eng. Leonardo Bozzoli, Eng. Francesco Muscatello and Eng. Francesca Sopranzetti at Alstom Ferroviaria SpA for having made this research possible. The authors would also like to acknowledge Eng. Francesco Vai, laboratory director at the Department of Industrial Engineering, University of Bologna, for his fundamental contribution to the experimental activities.

REFERENCES

[1]-Niemann G, Winter H, Hohn BR. Maschinenelemente: Band 1: Konstruktion und Berechnung von Verbindungen, Lagern, Wellen, Springer-Verlag: Berlin, Germany, 2005.

[2]-De Agostinis M, Fini S, Olmi G. The influence of lubrication on the frictional characteristics of threaded joints for planetary gearboxes. Proceedings of the Institution of Mechanical Engineers. Part C: Journal of Mechanical Engineering Science, 230 (15), 2553-2563.

[3]-UNI EN 10025-2, 2005, Hot rolled products of structural steels, Part 2: Technical delivery conditions for non-alloy structural steels.

[4]-UNI EN 1993-1-8, 2005. Eurocode 3, Design of steel structures, Part 1-8: Design of joints.

[5]-Croccolo; D. De Agostinis; M. Vincenzi, N. Structural analysis of an articulated urban bus chassis via FEM: a methodology applied to a case study, *Strojnicki Vestnik Journal of Mechanical Engineering*, vol. 57 (11),799-809.

[6]-UNI EN 10478-1, 1996, Non Destructive Testing - Inspection by strain gauges: Terms and definitions.

[7]-UNI EN 10478-2, 1998, Non Destructive Testing - Inspection by strain gauges: Selection of strain gauges and accessory components.

[8]-UNI EN 10478-3, 1998, Non Destructive Testing - Inspection by strain gauges: Strain gauge installation and checking.

[9]-ISO 8734, 1997, Parallel pins, of hardened steel and martensitic stainless steel (Dowel pins).

[10]-Croccolo, D. De Agostinis, M. Fini, S. Olmi, G. Tribological properties of bolts depending on different screw coatings and lubrications: An experimental study, *Tribology International* 107, 199-205.

[10]-De Agostinis, M. Fini, S. Olmi, G. The influence of lubrication on the frictional characteristics of threaded joints for planetary gearboxes, *Proceedings of the Institution of Mechanical Engineers, Part C: Journal of Mechanical Engineering Science* 230 (15), 2553-2563.

[12]-Eccles, W. Sherrington, I. Arnell, R.D. Frictional changes during repeated tightening of zinc plated threaded fasteners, *Tribology International* 43 (2010) 700-707.

[13]-ISO 898-1, 2009, Mechanical properties of fasteners made of carbon steel and alloy steel - Part 1: Bolts, screws and studs with specified property classes - Coarse thread and fine pitch thread.